Chemistry & Biology
Article

# Molecular Identification of Albumin and Hsp70 as Cytosolic Anandamide-Binding Proteins

Sergio Oddi,[1,2] Filomena Fezza,[2,3] Nicoletta Pasquariello,[1] Antonella D'Agostino,[1] Giuseppina Catanzaro,[1,2] Chiara De Simone,[2,3] Cinzia Rapino,[1] Alessandro Finazzi-Agrò,[3] and Mauro Maccarrone[1,2,*]
[1]Department of Biomedical Sciences, University of Teramo, Teramo 64100, Italy
[2]Santa Lucia Foundation I.R.C.C.S., Rome 00143, Italy
[3]Department of Experimental Medicine and Biochemical Sciences, University of Rome "Tor Vergata," Rome 00133, Italy
*Correspondence: mmaccarrone@unite.it
DOI 10.1016/j.chembiol.2009.05.004

## SUMMARY

**The cellular uptake and the intracellular synthesis/degradation of anandamide are crucial steps for controlling its extracellular level and the duration of its activity. Although the biosynthesis and breakdown of anandamide are well understood, little is known about the mechanisms underlying its intracellular transport. Here, we investigated the presence of a potential carrier-mediated trafficking of anandamide within the cytosol, using a biotinylated analog as a tool to catch by affinity chromatography anandamide-interacting proteins. The identity of two of these anandamide-binding proteins, Hsp70 and serum albumin, was determined by mass spectrometry, confirmed by western blotting and confocal microscopy, and further validated through an anandamide-binding assay. These findings suggest that the trafficking of anandamide from the plasma membrane to the internal compartments of a cell occur via a nonvesicular mechanism mediated by cytosolic carriers.**

## INTRODUCTION

The endogenous cannabinoid anandamide (*N*-arachidonoylethanolamide, AEA) has been implicated as a local mediator in several functions, including proliferation, growth arrest, differentiation, and death of the cells (Berghuis et al., 2005; Casanova et al., 2003; Maccarrone et al., 2003; Paradisi et al., 2008). Like the pharmacologically active lipids present in *Cannabis sativa* preparations, AEA elicits its effects primarily through specific plasma membrane receptors, including type 1 and type 2 cannabinoid receptors (CB1R and CB2R) (Matsuda et al., 1990; Munro et al., 1993), and possibly GPR55, a purported CB3 receptor (Lauckner et al., 2008). CB1R and CB2R are expressed in almost all of the body's districts. Moreover, AEA also acts as a true endovanilloid by binding the transient receptor potential vanilloid 1 (Starowicz et al., 2007), and as a ligand of the $\alpha$ and $\gamma$ isoforms of the nuclear peroxisome proliferator-activated receptors (PPARs) (Sun and Bennett, 2007). Thus, it is not surprising that a modulatory role of AEA has been demonstrated in the nervous, immune, cardiovascular, and reproductive systems (Di Marzo, 2008; Klein, 2005; Piomelli, 2003; Wang et al., 2006).

Like for most paracrine mediators, the action of AEA is determined by its extracellular concentration that is controlled, in turn, by the rate of its synthesis and degradation. Because both biosynthetic and hydrolytic enzymes, *N*-acylphosphatidylethanolamine (NAPE)-hydrolyzing phospholipase D (NAPE-PLD) and fatty acid amide hydrolase (FAAH), respectively, are intracellularly located (Desarnaud et al., 1995; Oddi et al., 2005; Ueda et al., 2005), a transport system for the rapid and efficient trafficking of AEA from and to these topographically separated sites can be expected. Several studies supported the notion that the migration of extracellular AEA within the cell is indeed a multistep process that consists of at least four phases: (i) adsorption to the plasma membrane, (ii) transmembrane movement, (iii) desorption from the plasma membrane, and (iv) intracellular trafficking, accumulation, and hydrolysis (Glaser et al., 2005; McFarland and Barker, 2004). At present, there is considerable controversy regarding the first two events—the binding to, and the transport across, the plasma membrane—because it is not yet established whether they occur via a protein-dependent or independent mechanism (Fegley et al., 2004; Fowler et al., 2004; Glaser et al., 2003; Kaczocha et al., 2006; McFarland et al., 2004; Moore et al., 2005). In any case, the intracellular transport of AEA, which is slow because of the low solubility of this compound in water, should be facilitated by a transport system, which likely involves either vesicles or soluble carrier proteins, or a combination of the two (Deutsch et al., 2001; Fowler et al., 2004; Glaser et al., 2003; Hillard and Jarrahian, 2003; McFarland et al., 2004; Ortega-Gutierrez et al., 2004; Ruiz-Llorente et al., 2004). Although some evidence in support of a vesicular pathway involving caveolae-related endocytosis (McFarland et al., 2004) and lipid droplets (Oddi et al., 2008) has been presented, as yet no direct evidence exists for a nonvesicular transport mediated by cytosolic carrier(s) specific for AEA.

To explore the possibility that AEA intracellular transporter(s) are present in the cytosol, we recently developed and characterized a biotinylated analog of AEA, b-AEA (Fezza et al., 2008; Oddi et al., 2008), which fully mimics the transport and intracellular accumulation of AEA (Fezza et al., 2008; Oddi et al., 2008). Here, b-AEA was used as a "bait" for affinity purification using avidin-based chromatography of AEA-interacting molecules from extracts of murine keratinocyte cytosols. The AEA-binding proteins were separated by multidimensional PAGE and were identified by mass spectrometry (MS). Using these approaches, we identified two proteins, serum albumin and heat shock protein 70.2 (Hsp70.2), as cytosolic AEA-binding proteins, thus

 

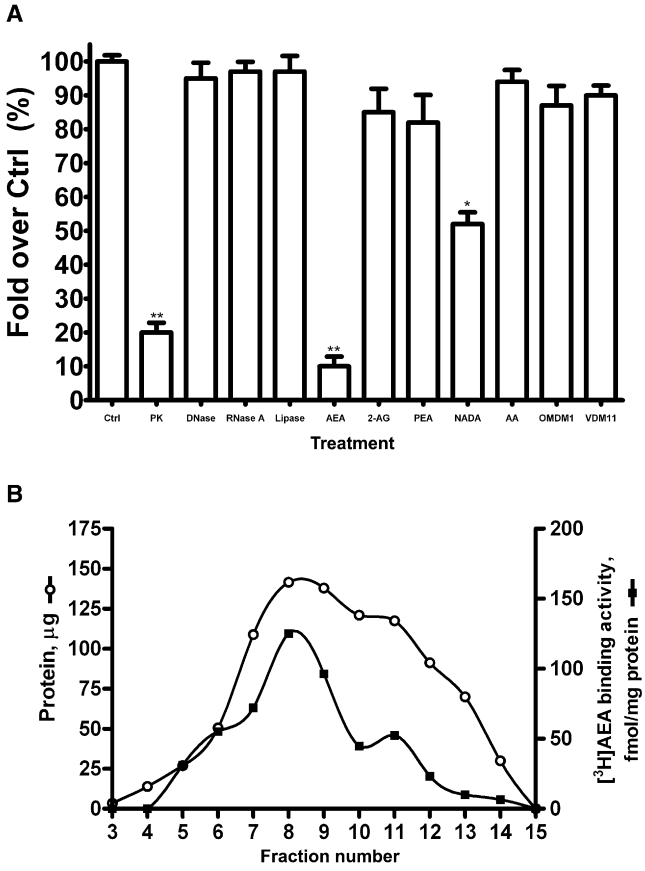


**Figure 1. Identification of AEA-Binding Sites within the Cytoplasm**

(A) Analysis of the molecular nature and substrate specificity of the [$^3$H]AEA-binding sites in the cytosolic fractions of mouse keratinocytes. Cytosolic preparations were incubated with 2 nM [$^3$H]AEA and then incubated with protease K (PK), DNase I (DNase), RNase A, pancreatic lipase C (Lipase), unlabelled AEA, 2-arachidonoylglycerol (2-AG), *N*-palmitoylethanolamine (PEA), *N*-arachidonoyldopamine (NADA), arachidonic acid (AA), or two AEA uptake inhibitors, OMDM1 and VDM11. Results are expressed as percentage of untreated cytosol (Ctrl, 100% = 68 ± 5 fmol/mg protein).*$p < 0.05$ versus Ctrl; **$p < 0.01$ versus Ctrl. Error bars represent standard error of the mean (SEM) of at least two independent experiments, each performed in triplicate. (B) Partial purification of AEA-binding proteins by gel-filtration chromatography. Cytosolic extracts were eluted on a gel-filtration column (Zorbax GF-450), and the resulting fractions were analyzed for protein content (○) and [$^3$H]AEA-binding activity (■).

providing the first evidence for the presence of a nonvesicular mechanism involved in the intracellular trafficking of anandamide.

## RESULTS

### Identification of AEA-Binding Activity within the Cytosol

In preliminary experiments, we attempted to determine if the epidermal cytosol contained AEA-binding sites. We found that cytosol preparations could bind this endocannabinoid up to about 70 fmol/mg protein. The protein nature of the AEA-binding sites was indicated by their susceptibility to proteolytic digestion by protease K and their resistance to DNase I, ribonuclease A, and pancreatic lipase (Figure 1A).

In order to investigate the specificity of the AEA-binding activity, competitive experiments were performed. Cytosol preparations were incubated with [$^3$H]AEA (2 nM) in the presence of a 50-fold excess of structurally related, unlabelled compounds (Figure 1A). As expected, the binding of 2 nM [$^3$H]AEA to cytosolic protein(s) was reduced (down to ~10%) by an excess of unlabelled AEA. A less pronounced, yet significant, ~50% displacement was observed using the AEA congener *N*-arachidonoyldopamine. However, 2-arachidonoylglycerol and *N*-palmitoylethanolamine could displace only ~15%–20% of the bound [$^3$H]AEA. Finally, arachidonic acid, a catabolic product of AEA, and two different AEA uptake inhibitors, (*S*)-1′-(4-hydroxybenzyl)-oleoylethanolamide (OMDM1) and *N*-(2-methyl-4-hydroxyphenyl)-arachidonamide (VDM11) (De Petrocellis et al., 2000; Ortar et al., 2003), showed only ~5% displacement of bound [$^3$H]AEA (Figure 1A). These results suggest the presence of AEA-binding proteins within the cytosol, which appear to be different from those that are responsible for the transport of AEA across the plasma membrane.

### Gel Filtration and [$^3$H]AEA-Binding Activity

Analysis of the fractions derived from a gel filtration column suggested that [$^3$H]AEA eluted after 17 min (Figure 1B) with an elution profile only partially superimposable to that of the cytosolic proteins, indicating that AEA was primarily associated with specific protein(s) with an apparent molecular weight of 63 ± 25 kDa (Figure 1B and Table 1). Interestingly, the presence of a shoulder in the elution profile (fraction 6) and of a minor peak in fraction 11 were also noted, suggesting that AEA might bind to a variety of cytosolic proteins ranging from ~660 kDa to < 43 kDa. However, only the most active fractions (7–9) were further analyzed in this study.

### Nano-LC ESI-MS/MS Identification of Affinity-Purified AEA-Binding Proteins

The most AEA-binding-rich fractions (7–9), amounting to ~65% of the total AEA-binding activity, were pooled, labeled by incubation with 20 µM b-AEA for 1 hr, and loaded onto a monomeric avidin column for further purification by affinity chromatography. The b-AEA-binding molecules retained by avidin were then eluted by competition with biotin. Then, such proteins were further separated by 2D PAGE (Figure 2). By comparing the 2D PAGE profiles of the affinity-purified samples with a mock-purified control (Figure 2A), we identified several specific spots (Figure 2B). Among these, we focused on three major spots (labeled 4, 5, and 6) of apparent molecular mass of ~50–70 kDa. Our analysis did not include low abundance protein spots because of anticipated difficulties in obtaining satisfactory protein identification by MS. These spots were excised from the gel for tryptic digestion, and the resulting peptides were analyzed by nano-liquid chromatography electrospray ionization tandem mass spectrometry (nano-LC ESI-MS/MS). Peptide masses were searched using the Mascot engine with a tolerance of 300 ppm (for more details on MS spectra, see Supplemental Data available online). The database search resulted in heat shock protein 70.2 (Hsp70.2) (spot 4; pI = 5.58; Mr = 69,684 Da), with 6% sequence coverage (number of peaks matched = 3) and a Mowse score of 82 ($p < 0.05$; Figure 2D), and serum albumin (spot 5; pI = 5.75 ; Mr = 68648 Da), with 2% sequence coverage

**Table 1. Purification of Intracellular Anandamide-Binding Sites from Skin Keratinocytes**

| Fraction | Total Activity (fmol [$^3$H]AEA) | Protein (μg) | Specific Activity (fmol [$^3$H]AEA/mg) |
|---|---|---|---|
| Cytosol | 60.8 | 0.9 | 67.5 |
| 1 | ND[a] | ND | ND |
| 2 | ND | ND | ND |
| 3 | ND | 3.4 | ND |
| 4 | ND | 13.9 | ND |
| 5 | 0.8 | 26.9 | 29.7 |
| 6 | 2.8 | 50.6 | 55.3 |
| 7 | 7.8 | 108.9 | 71.6 |
| 8 | 17.7 | 141.5 | 125.1 |
| 9 | 13.3 | 137.9 | 96.4 |
| 10 | 5.4 | 120.9 | 44.7 |
| 11 | 6.2 | 117.4 | 52.8 |
| 12 | 2.1 | 91.2 | 23.0 |
| 13 | 0.7 | 70.0 | 10.0 |
| 14 | 0.2 | 30.1 | 6.6 |
| 15 | ND | 2.0 | ND |

[a] ND indicates not detectable

(number of peaks matched = 1) and a Mowse score of 90 ($p < 0.05$; Figure 2C). The analysis of spot 6 led to a protein score of 35 and therefore its identity remained elusive. It is important to note that the MS analysis of each spot led to fragments belonging to single proteins, suggesting that the analyzed spots contained only a single protein. The coordinates (molecular mass and pI) of the detected spots were estimated by interpolation with standard proteins, and were in good agreement with the nominal mass and calculated isoelectric point values of the proteins identified by MS (Figure 2B and Table 2). Notably, serum albumin has been described to bind AEA in vitro with high affinity (Bojesen and Hansen, 2003; Giuffrida et al., 2000), thus supporting our proteomic analysis. The results of the MS analysis were confirmed by western blotting analysis of the affinity-purified sample, performed using commercially available antibodies against Hsp70 and serum albumin (Figure 2E). Moreover, we confirmed by confocal microscopy the expression and the intracellular localization of both Hsp70 and serum albumin in epidermal keratinocytes (data not shown). Although our MS data, together with the experimental molecular mass and pI, point toward Hsp70.2, which is constitutively expressed in the cell cytoplasm in most tissues, including epidermis, it could not be excluded that other members of Hsp70 family—a group of highly related chaperonins that have remarkable sequence identity—might bind AEA, likely through their well-conserved binding domains.

### In Vitro Analysis of Hsp70-AEA Interaction

In order to confirm the physical interaction between Hsp70.2 and AEA, we developed a straightforward method consisting of a "pull-down" assay adapted for protein-lipid interaction studies. Hsp70.2 is highly conserved between human and mouse, showing remarkable homology with 96% amino acid identity. Human and mouse serum albumin is also very conserved, with over 71% identity. Therefore, these high levels of identity allowed us to shift our study from mouse to human models. After 1 hr incubation at various [$^3$H]AEA concentrations, AEA binding to human Hsp70 was determined by counting the radioactivity retained by the resin-bound proteins. The procedure was first validated by analyzing AEA affinity for human serum albumin (HSA), because it is known that albumin binds AEA with a Kd value in the nanomolar range at 23°C (Bojesen and Hansen, 2003; Giuffrida et al., 2000). We found that although the resin per se did not retain a significant amount of radioactivity, 15 nmol resin-adsorbed HSA was able to bind [$^3$H]AEA in a concentration-dependent manner, typical of a saturable process (Figure 3A), with apparent Kd and Bmax values of 0.8 ± 0.1 μM and 2.3 ± 0.2 nmol/mg protein, respectively. Next, the assay for the detection of Hsp70-AEA complexes was carried out with 12 nmol resin-bound protein. As shown in Figure 3B, AEA exhibited saturable binding also to Hsp70. The experimental data were fitted to a rectangular hyperbola with an apparent Kd value of 3.7 ± 0.5 μM and a Bmax of 1.9 ± 0.1 nmol/mg protein, indicating that Hsp70 binds AEA with a ~5-fold lower affinity than HSA.

### Effect of Hsp70 Overexpression on AEA Uptake in SH-SY5Y Cells

Because primary keratinocytes transfected with relatively poor efficiency (<5%) (Leask et al., 1990), we assessed the effect of Hsp70.2 overexpression on AEA uptake in human neuroblastoma SH-SY5Y cells transiently transfected with the expression vector pcDNA-human Hsp70.2. After 24 hr, expression levels of Hsp70.2 in the cells were assessed by immunofluorescence, using an anti-Hsp70 antibody. Transfection efficiency, measured as percentage of Hsp70.2-overexpressing cells, was ~50% (data not shown). We found that the overexpression of Hsp70.2 increased ~5-fold [$^3$H]AEA uptake, from 0.40 ± 0.10 pmol/min per mg protein in mock-transfected cells to 2.12 ± 0.20 pmol/min per mg protein in Hsp70.2-transfected cells (mean ± SEM; $n = 6$; $p < 0.0001$) (Figure 3C). As a control, the addition of 5 μM OMDM-1 minimized the transport of AEA across the cell membrane (Figure 3C).

Consistently with the affinity purification data, coimmunostaining of exogenous Hsp70.2 and b-AEA showed a marked colocalization of the two molecules (Figures 3D–3F). As indicated in the merged picture (Figure 3F, arrowheads in the inset), an array of b-AEA-positive tubular structures was also positive for Hsp70.2. Moreover, a diffuse cytosolic distribution for both substances was observed. Interestingly, tubular structures with both Hsp70.2 and b-AEA stainings were observed in the close proximity of plasma membrane (Figure 3D–3F, asterisks), suggesting a potential interaction between these two molecules also at the level of the cell membrane. Altogether, these experiments indicate that Hsp70.2 enhances the rate of the cellular uptake of AEA, possibly as a result of its direct interaction with this lipid.

## DISCUSSION

Recently, increasing attention has been directed toward AEA transport across the cell membrane, because of its role in the regulation of the biological activity of AEA (Dainese et al., 2007; Fowler et al., 2005; McFarland and Barker, 2004). However, despite its pathophysiological relevance, there is as yet no

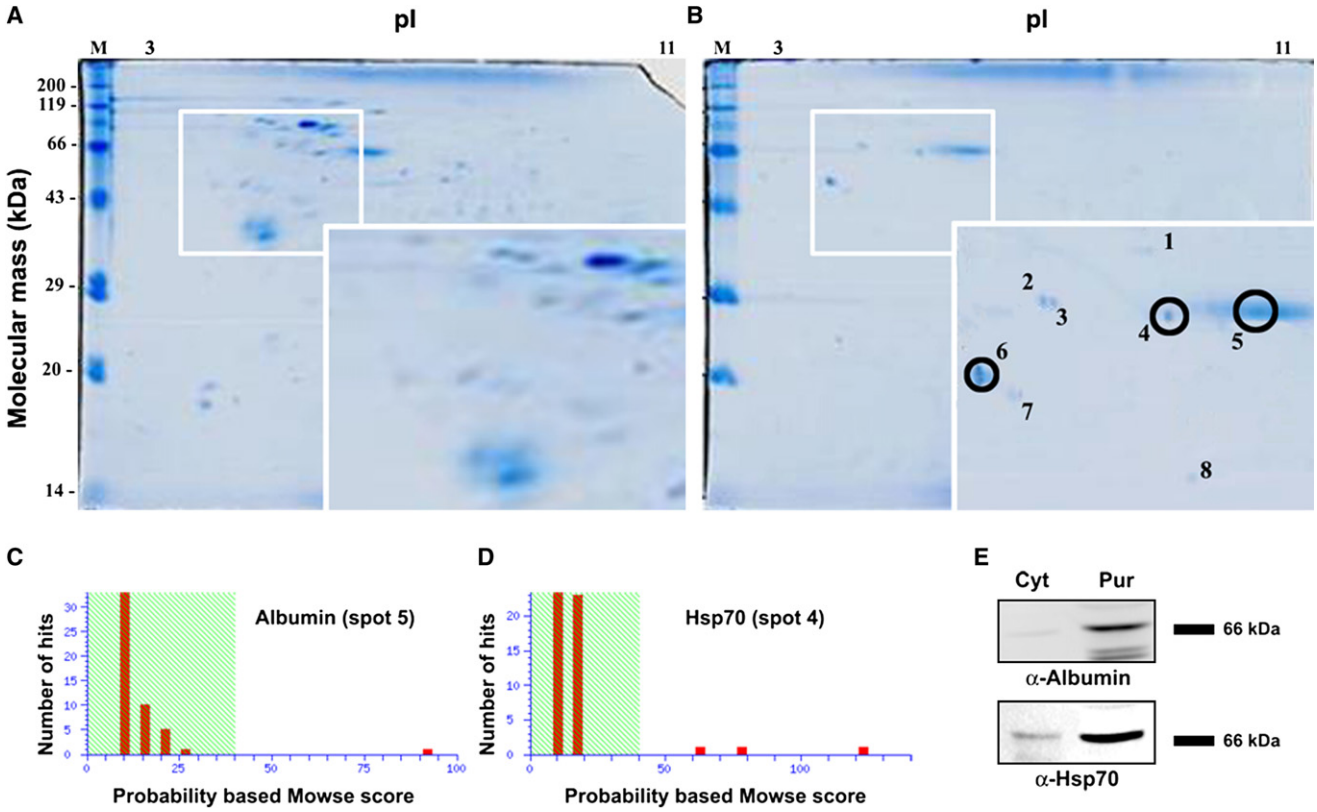


**Figure 2. Gel Electrophoresis and Mass Spectrometry Identification of the Affinity-Purified AEA-Binding Proteins**

(A–D) Representative bidimensional electrophoresis (2D-PAGE) gels of mock-purified (A) and affinity-purified (B) samples. Nonspecifically and specifically eluted proteins were resolved by 2D-PAGE on nonlinear pH 3–11 isoelectrofocusing strips, followed by separation on a 12% SDS-PAGE gel in the second dimension. Proteins were visualized by colloidal Coomassie staining. In the insets, high-magnification views of the gels of a selected area are shown. Circled spots indicate proteins further subjected to mass spectrometry. Mascot search results and probability plots corresponding to albumin (C) and Hsp70 (D).

(E) Western blotting analysis of cytosol (cyt) and affinity-purified sample (Pur), using antibodies against serum albumin and Hsp70.

consensus on how this process occurs, i.e., by (i) passive diffusion, (ii) facilitated diffusion, or (iii) a combination of both. Another ill-defined issue is the mechanism whereby AEA detaches from the plasma membrane and, subsequently, diffuses throughout the cytoplasm, a process that is likely to represent the bottleneck of AEA metabolism (Forneris and Mattevi, 2008). Although AEA, a neutral lipid, is sufficiently lipophilic to partition into the membrane bilayers (log p = 5.1 [Oddi et al., 2008]), a simple, non-ordered diffusion of AEA through the aqueous cytoplasm to intracellularly located targets is unlikely to be fast enough to account for the rate and the extent of intracellular accumulation and metabolism of this endocannabinoid (Beltramo et al., 1997; Hillard and Jarrahian, 2000; Jacobsson and Fowler, 2001; Maccarrone et al., 2000; Ortega-Gutierrez et al., 2004; Rakhshan et al., 2000). From this point of view, an "organized system" has been hypothesized for the efficient delivery of AEA to its hydrolase FAAH, and/or to other potential internal targets (Hillard and Jarrahian, 2003). Experimental evidence in support of such an organized system has been indeed provided, suggesting the involvement of a lipid rafts/caveolae endocytic pathway for the transmembrane transport of AEA, as well as for its recycling after catabolism (McFarland et al., 2004). Moreover, a dynamic interaction has been recently described between AEA and adiposomes, lipid storage vesicles that could act as shuttles for the transport of this lipid among intracellular compartments (Oddi et al., 2008). Another unexplored possibility is that some soluble proteins ferry AEA through the cytoplasm; this could speed up its internalization, by analogy with what observed for

**Table 2. MS/MS-Identified Proteins in Affinity-Purified Samples**

| Spot Number | Accession Number | Protein | Molecular Mass (kDa) (Theoretical/ Experimental) | Isoelectric Point (Theoretical/ Experimental) | MASCOT Score | Peptides Matched | Sequence Coverage (%) | MS/MS Sequences |
|---|---|---|---|---|---|---|---|---|
| 4 | gi\|123621 | HSP70.2 | 69.7/67 | 5.58/5.0 | 82 | 3 | 6 | R.IINEPTAAAIAYGLDK.K<br>R.FEELNADLFR.G<br>R.VAAKNAVESYTYNIK.Q |
| 5 | gi\|163310765 | Albumin | 68.7/67 | 5.75/5.2 | 90 | 1 | 2 | K.LGEYGFQNAILVR.Y |

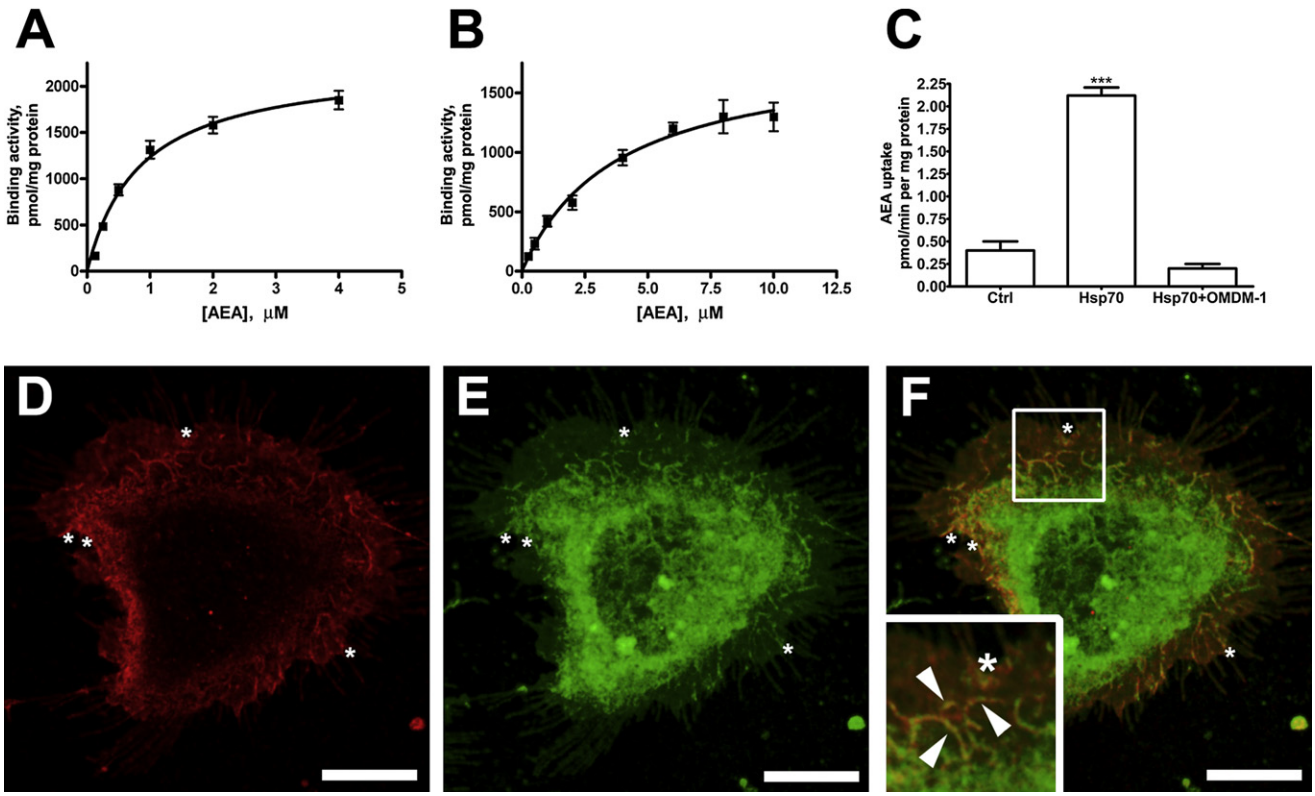


**Figure 3. AEA-Binding of Serum Albumin and Hsp70**

(A and B) AEA binding to 5 μg albumin (A) or Hsp70 (B) immobilized to 10 μl resin was determined by means of a batch method. The resin-adsorbed proteins were incubated with varying concentrations of AEA for 30 min at 25°C. Nonspecific adsorption of AEA to cellular membranes or cell supports was estimated by running the identical experiments at 4°C, and was subtracted from each data point. The lines drawn are the best fit of the data to one-site-binding hyperbola. Values are means ± SEM of at least two independent experiments, each performed in triplicate. Overexpression of Hsp70.2 in SH-SY5Y cells.

(C) Effect of Hsp70.2 overexpression (Hsp70) versus control (Ctrl) on [$^3$H]AEA uptake by SH-SY5Y cells, grown in the absence or in the presence of 5 μM OMDM1 (Hsp70 + OMDM-1). ***$p < 0.0001$ versus Ctrl.

(D–F) Double immunofluorescence of Hsp70.2 (red) and b-AEA (green). The superimposition of the two stainings revealed that Hsp70.2 and b-AEA colocalize in tubular structures within the cytosol (arrowheads in the inset) or near to the plasma membrane (asterisks). The images are representative of three independent experiments, and in each case five fields were examined. Scale bar, 10 μm.

other lipids, including cholesterol (Soccio and Breslow, 2004), ceramide (Hanada et al., 2003), and long-chain fatty acids (Furuhashi and Hotamisligil, 2008). However, so far no evidence exists for such a nonvesicular transport of AEA, primarily because of methodological limitations in studying the movement of AEA by the current radiometric-based techniques (Glaser et al., 2005).

In the present study we sought to address this issue by employing a biotinylated analog of AEA, b-AEA (Fezza et al., 2008; Oddi et al., 2008), as a valuable affinity chromatography tool. Based on the well-characterized presence of the endocannabinoid system in the epidermis (Casanova et al., 2003; Maccarrone et al., 2003; Paradisi et al., 2008), we decided to use keratinocytes as an experimental model to explore the presence of constitutive intracellular AEA transporters. Moreover, because epidermis is an avascular tissue mostly made of cells with poor extracellular space (Fuchs, 1990), mouse epidermal keratinocytes represent a convenient source of cytosolic proteins virtually devoid of any contamination from blood proteins. In preliminary experiments, we found that the cytosolic extracts contained a specific AEA-binding activity associated with proteins and insensitive to OMDM1 and VDM11, two well-characterized inhibitors of AEA uptake (De Petrocellis et al., 2000; Ortar et al., 2003), suggesting that the cytosolic proteins involved in intracellular AEA binding were different from those that are responsible for the transmembrane transport of AEA. Interestingly, we found that AEA binding was specifically inhibited by *N*-arachidonoyldopamine (NADA) but not by 2-arachidonoylglycerol, palmitoylethanolamine (PEA), or arachidonic acid, indicating that ligand recognition by the cytosolic AEA carrier(s) implies stringent structural determinants.

Next, by using affinity chromatography, we were able to isolate several AEA-interacting proteins in the cytosolic extract from mouse epidermal keratinocytes. Among these, we identified by MS the proteins corresponding to two major spots: serum albumin and Hsp70.2. The identity of these proteins was subsequently confirmed by western blotting and immunofluorescence. Concerning albumin, among the albuminoid gene family, consisting of serum albumin (69.7 kDa), alpha-fetoprotein (47 kDa), vitamin D binding protein, and alpha-albumin (afamin), only alpha-fetoprotein and serum albumin match with the MS-identified peptide. Considering the experimental molecular mass of

the protein spot (67 kDa), we concluded that the analyzed spot consists of serum albumin and not of alpha-fetoprotein. However, due to their high homology, it could not be excluded that alpha-fetoprotein might bind AEA. Albumin has been demonstrated to bind AEA with high affinity in the extracellular milieu (Bojesen and Hansen, 2003; Giuffrida et al., 2000), but this is the first evidence that endogenous albumin interacts with AEA within the cell. In fact, until now serum albumin has been shown to bind and transport AEA only in blood, whereas a role for albumin in the cytoplasm has not been considered. In this context, it seems noteworthy that the endogenous synthesis of albumin in human epidermis, as well as in human keratinocytes in culture, has been previously documented both at transcriptional and translational level (Hasse et al., 2005; Katz et al., 1970; Rabilloud et al., 1988). In agreement with these studies, we confirmed by western blotting and confocal microscopy the expression and the intracellular localization of albumin in epidermal keratinocytes, indicating that AEA-binding albumin was endogenously expressed, and was not a contaminant from serum. Therefore, besides binding and transporting AEA in plasma and in the extracellular space, albumin seems to act also as an intracellular AEA transporter (AIT). Taking into account that variable levels of albumin have been found within the cytosol of different cell lines, and that this protein is particularly expressed in actively metabolizing or developing tissues, it could be proposed that albumin has a role in controlling the bioavailability of AEA in multiple functional contexts. At present, very few information exists regarding the structural aspects of the interactions between HSA and AEA. As ethanolamide of arachidonic acid, AEA binds to albumin in only one high-affinity binding site (Bojesen and Hansen, 2003), with a somewhat lower binding constant than that seen for arachidonic acid, which, unlike AEA, can bind to albumin at three different binding sites. These differences have been imputed to the fact that AEA is not only a neutral molecule but it is also much larger than arachidonic acid. However, a complete and reliable assignment of the AEA-binding site on albumin is unsettled and will require further work.

The human Hsp70 family comprises at least eight unique gene products that differ from each other by amino acid sequence, expression level, and subcellular localization. Our MS data, together with the experimental molecular mass and pI, point toward Hsp70.2, which is constitutively expressed in the cell cytoplasm in most tissues, including epidermis. However, as stated for albumin, because Hsp70.2 shows high homology with other members of Hsp70 family (for example, it displays 86% identity to heat shock cognate 70), it could not be excluded that other members of this family might bind AEA, through their conserved binding domains. In order to confirm the interaction between Hsp70 and AEA, we developed an in vitro batch method that has the limitation of recording AEA/Hsp70 complex formation after several washing steps, and thus not at equilibrium. Consequently, the observed Kd and Bmax were only rough estimates of the actual binding parameters. By utilizing pure proteins, we found that Hsp70, alike HSA, was able to bind AEA in a concentration-dependent manner, typical of a saturable process, though with a lower affinity than HSA. More sophisticated techniques, such as calorimetry (Gazzara et al., 1997), surface chemistry (Ibdah et al., 1989), capillary electrophoresis (Breyer et al., 2003), or resonance energy transfer (Drin et al., 2001), should be adapted in order to better quantify the binding properties of Hsp70 toward AEA, and hence its suitability as a physiological AIT. In this context, Hsp70 is able to interact with lipids, including sterols and sphingolipids (Gacad and Adams, 1998; Mamelak and Lingwood, 1997), through a binding site that has been localized in the conserved, N-terminal ATPase-containing domain (Mamelak and Lingwood, 1997). Moreover, similar to other members of its family, Hsp70 is not exclusively localized within the cytosol, but has also been found in association with membrane lipids (Gehrmann et al., 2008; Uittenbogaard et al., 1998). Here, we confirmed the intracellular localization of Hsp70.2 by confocal microscopy, showing that it has a predominant cytoplasmic staining partially overlapped to that of b-AEA. In addition, we also observed costaining of Hsp70.2 and b-AEA close to the plasma membrane, suggesting that Hsp70.2 might interact with AEA also at this level.

During the revision process of this manuscript, a paper appeared describing fatty-acid-binding proteins that, when overexpressed, behave as intracellular proteins that bind AEA, complementing the findings of our study (Kaczocha et al., 2009).

## SIGNIFICANCE

**Due to their role in the regulation of the extracellular tone of AEA, both cellular uptake and metabolism of AEA are crucial steps for controlling the duration of its activity, and thereby represent potential targets for the development of therapeutic strategies aimed at modulating the level of AEA in several pathologies. Although the biosynthesis and breakdown of AEA were well understood, very little is known about the mechanisms underlying its intracellular transport. Herein we investigated the presence of a potential carrier-mediated trafficking of AEA within the cytosol, using a biotinylated analog of AEA, biotin-AEA, as a "bait" to isolate by affinity chromatography its endogenous interacting proteins. From the above-mentioned findings, it is conceivable that Hsp70, perhaps assisted by serum albumin, may act as an AIT in the cytosol, and as an "AEA chaperon" at the plasma membrane, where it might promote the desorption of this lipid, thus facilitating its transport through the cytoplasm. Then, AEA can be delivered to specific compartments within the cell, for example to the lipid droplets for accumulation, to the endoplasmic reticulum for degradation (via FAAH), or to the nucleus for transcriptional regulation (via PPAR-$\alpha/\gamma$).**

**In summary, this work provides the first evidence for the existence of AEA intracellular transporters, which might form a delivery system active in cytosol, plasma membrane, nucleus, and endoplasmic reticulum, to rapidly and efficiently assist the intracellular trafficking of AEA.**

## EXPERIMENTAL PROCEDURES

### Reagents

All chemicals were of the purest analytical grade. [$^3$H]AEA (205 Ci/mmol) was from Perkin-Elmer Life Sciences (Boston, MA). AEA, HSA, bovine serum albumin, human Hsp70 (cod. H7283) and the anion-exchange resin diethylaminoethyl (DEAE)-Sepharose were from Sigma Chemical (St. Louis, MO). PEA and NADA were from Tocris Cookson (Bristol, UK). Arachidonic acid, OMDM1, and VDM11 were purchased from Cayman Chemical (Ann Arbor, MI). The biotinylated analog of AEA, b-AEA, was synthesized and purified as

described elsewhere (Fezza et al., 2008). YM-10 Centricon devices were purchased from Millipore Co. (Rome, Italy). Rabbit anti-Hsp70 (cod. sc-33575) and anti-albumin (cod. sc-46290) polyclonal antibodies were obtained from Santa Cruz Biotechnology (Santa Cruz, CA). Mouse anti-biotin monoclonal antibody, goat Alexa Fluor-conjugated secondary antibody, and Prolong anti-fade kit were purchased from Molecular Probes (Eugene, OR). The plasmid expressing human Hsp70.2 (pcDNA3-Hsp70.2) was a kind gift of Dr. Antonio Rossi of the Institute of Neurobiology and Molecular Medicine (National Research Council, Rome, Italy). LipofectAMINE 2000 was from Invitrogen Life Technologies. Culture media, sera, and supplements were obtained from PromoCell (Heidelberg, Germany). All other chemicals were from Sigma Chemical, unless otherwise indicated.

### Epidermal Explantation

Twenty-five newborn mice (1–2 days old) were killed by cervical dislocation after anesthesia and the skin was removed, rinsed in $Ca^{2+}/Mg^{2+}$-free phosphate-buffered saline (PBS), and incubated in 1% trypsin in PBS for 18 hr at 4°C. Explanted skins were transferred to PBS at room temperature (RT) and aspirated with a Pasteur pipette to loosen the epidermis, which was subsequently removed, using forceps and a tungsten needle, and extensively washed with ice-cold PBS.

### Extraction of Cytosolic Proteins

To isolate cytosolic proteins, epidermal mouse keratinocytes were explanted from the skin of newborn mice. To this end, 25 newborn mice (1–2 days old) were killed by cervical dislocation after anesthesia and the skin was removed, rinsed in $Ca^{2+}/Mg^{2+}$-free PBS, and incubated in 1% trypsin in PBS for 18 hr at 4°C. Explanted skins were transferred to PBS at RT and aspirated with a Pasteur pipette to loosen the epidermis, which was subsequently removed, using forceps and a tungsten needle, and extensively washed with ice-cold PBS. The cell extracts were resuspended in hypotonic buffer (5 mM Tris-HCl [pH 7.4], 10 mM KCl, 5 mM EDTA, 1 mM 4-[2-aminoethyl]benzenesulfonyl fluoride, and 1 mM DTT) and lysed on ice using a loose-fitting Dounce homogenizer. After low-speed centrifugation to remove nuclei and intact cells, the cytosolic fraction was prepared by centrifuging supernatants at 250,000 x *g* for 2 hr at 4°C. The cytosol samples were dialyzed against PBS for 5 hr at 4°C, and the protein concentration was measured by the Bradford assay kit (Bio-Rad, Hercules, CA).

### [$^3$H]AEA-Binding Assay by Ultrafiltration

The estimation of AEA binding to cytosol extracts was performed by adapting a method based on centrifugal ultrafiltration (Menguy et al., 1998). In a typical binding experiment, 0.5 ml cytosol samples containing 1.5 mg protein/ml were incubated with an equal volume of [$^3$H]AEA in PBS (final concentration, 2 nM; specific activity, 205 Ci/mmol). The mixture was incubated for 30 min at RT. Preliminary experiments had shown that equilibrium was attained under these conditions. Nonspecific binding was checked by parallel incubations in the presence of a 200-fold molar excess of unlabelled AEA. After incubation, samples were rapidly filtered through YM-10 Centricon tubes (molecular weight cut-off, 10 kDa), to concentrate the macromolecules contained in the sample, while free [$^3$H]AEA flowed by. The retained fraction (100 μl) was then washed three times with PBS (5 ml per wash) to remove unbound [$^3$H]AEA. The amount of protein-bound AEA was calculated by measuring the radioactivity bound to the final concentrate. [$^3$H]AEA-binding activity was expressed as fmol [$^3$H]AEA bound per milligram protein. Due to variability between batches of Centricon devices, each lot was tested in the absence of proteins, to ensure that free AEA was efficiently flushed away after the washing steps. Each value was determined in triplicate and was corrected for nonspecific binding performed in parallel experiments. To test the sensitivity of [$^3$H]AEA binding in the cytosolic fraction to enzymatic digestion with protease K, DNase I, ribonuclease A, and pancreatic lipase, each enzyme was added to the samples at a concentration of 1 U/ml, and was incubated for 1 hr at 37°C. Then, [$^3$H]AEA binding was assayed as described above.

### Fractionation by Gel Filtration

Size-exclusion high-performance liquid chromatography measurements were performed on a PE Series 200 System (Perkin-Elmer) using a Zorbax GF-450 gel-filtration column (Agilent Technologies, Santa Clara, CA) that allows separation within a range from 10 to 1000 kDa. Cytosol (150 μl) was incubated with 2 nM [$^3$H]AEA and fractionated on the Zorbax GF-450 column using PBS as eluent, at RT and a flux rate of 1 ml/min. Protein concentration and radioactivity of the collected fractions were monitored using an ultraviolet-visible detector and a radiodetector, respectively. Protein size was determined by comparison with the following gel-filtration grade molecular mass standards (GE Healthcare, Uppsala, Sweden): ovalbumin (43 kDa), albumin (67 kDa), aldolase (158 kDa), and thyroglobulin (669 kDa).

### Biotin-Affinity Chromatography

The cytosolic fraction was preliminarily cleared of endogenous biotinylated proteins by passing through a monomeric avidin column (Pierce, Rockford, IL), equilibrated in PBS. The cleared extract was mixed with 20 μM b-AEA, incubated for 30 min at RT, and applied to freshly prepared monomeric avidin column. After sample application, the avidin column was washed extensively with PBS, until the absorbance value at 280 nm reached the baseline. Then, bound proteins were competitively eluted with PBS containing 2 mM biotin, and were concentrated on YM-10 Centricon filters for further analysis. Nonspecific elution from the affinity column was identified by collecting the eluate from the column loaded with cleared cytosol, but without added b-AEA.

### Two-Dimensional PAGE

2D-PAGE was performed using ready-made immobilized pH gradient (IPG) strip gels (7 cm IPG strips [pH 3–11]) from Bio-Rad. Each sample was applied onto an IPG gel by in-gel rehydration overnight. Isoelectric focusing was carried out in a Protean IEF cell apparatus (Bio-Rad), essentially as described elsewhere (Gorg et al., 2000). 2D-PAGE gels were stained with colloidal Coomassie (18% (v/v) ethanol, 15% (w/v) ammonium sulfate, 2% (v/v) phosphoric acid, 0.2% (w/v) Coomassie G-250) for 48 hr, and were destained with distilled water. Stained 2D-PAGE gels were scanned with ImageMaster VDS-CL (Amersham Biosciences, Uppsala, Sweden). Image analyses were performed using ImageMaster 2D Elite software (Amersham Biosciences). After spot detection, background subtraction was performed using mode of nonspot option, normalization was performed using total spot volume, and matching between gels of the same format was performed through user seeds match. For isoelectric point and molecular mass calibrations, the 2D-PAGE internal standards from Bio-Rad were used, performing IEF, SDS-PAGE, staining, and scanning as indicated above.

### Nano-LC ESI-MS/MS

Protein identification using nano-LC ESI-MS/MS was conducted by the Proteome Factory (Proteome Factory AG Berlin, Germany; http://www.proteomefactory.com). The MS system consists of an Agilent 1100 NanoLC system (Agilent, Germany), PicoTip emitter (New Objective, USA), and an Esquire 3000 plus ion trap MS (Bruker, Bremen, Germany). Protein spots were in-gel digested by trypsin (Promega, Mannheim, Germany) and applied to nano-LC-ESI-MSMS. After trapping and desalting the peptides on enrichment column (Zorbax SB C18, 0.3 × 5 mm, Agilent) using 1% acetonitrile/0.1% formic acid solution for 5 min, peptides were separated on Zorbax 300 SB C18, 75 μm × 150 mm column (Agilent) using an acetonitrile/0.1% formic acid gradient from 5% to 40% acetonitrile within 40 min. MS spectra were automatically taken by Esquire 3000 plus according to manufacturer's instrument settings for nano-LC-ESI-MS/MS analyses. The peptide mass mapping was performed on an ESI-TRAP, and was analyzed by LC-MS/MS. The matched peptides were searched using Mascot (http://www.matrixscience.co.uk), based on the NCBInr database and taking *Mus musculus* as the taxonomy. The searching parameters were: an MS/MS tolerance of ± 0.5 Da, one missed cleavage site, fixed modifications of carbamidomethyl, peptide tolerance of ± 0.5 Da, peptide charge of 1+ 2+ 3+, monoisotopic, and ESI-TRAP instrument. Probability-based Mowse scores were obtained using the same software, by comparing search results with an estimated random match population, and results were reported as $-10*\log(P)$, where P is the absolute probability. Individual ions scores greater than 40 indicate identity or extensive homology ($p < 0.05$). Protein scores were derived from ions scores as a non probabilistic basis for ranking protein hits. Only significant hits, as defined by the Mascot probability analysis ($p < 0.05$), were accepted. If multiple significant hits were found for a protein, only the highest scoring hit was listed in Table 2.

### Western Blotting

Cytosolic extracts (50 μl) and affinity purified sample (5% of the total amount) were subjected to western blotting according to standard procedures (Maccarrone et al., 2003), and serum albumin and Hsp70 were immunodetected using antibodies that are validated for detection of these proteins of both human and mouse origin.

### [$^3$H]AEA-Binding Assay by DEAE

For AEA-binding studies with HSA and Hsp70, a variant of the conventional pull-down assay was used. This method exploits the ability of DEAE resin to bind proteins but not free lipids. Purified and delipidated proteins (5 μg, corresponding to 15 nmol and 12 nmol HSA and Hsp70, respectively) were adsorbed to 30 μl slurry DEAE sepharose (50%, v/v) by incubating the suspension in 20 mM Tris-HCl (pH 7) for 15 min at RT. Then, DEAE-adsorbed proteins were incubated with various concentrations of [$^3$H]AEA for 1 hr at RT, and the suspension was vortexed every 10 min. The final volume was 200 μl, and the total concentration of methanol did not exceed 1%. At the end of the incubation, 1 ml ice-cold 20 mM Tris-HCl was added to stop the reaction, and the resin was collected by centrifuging at 7000 x *g* for 5 min, and washed twice in the same way. Then, DEAE was resuspended in 500 μl 20 mM Tris-HCl and added to a vial containing scintillation liquid, and radioactivity was measured in a beta-counter analyzer. Each value was determined in triplicate and was corrected against a blank (no protein added) assayed in parallel. The counts of blanks were never more than 7% of the total amount of ligand added. Binding data for HSA and Hsp70 were elaborated through nonlinear regression analysis, using the Prism 4 program (GraphPad Software Inc., San Diego, CA), in order to calculate apparent dissociation constant (Kd) and maximum binding (Bmax) of [$^3$H]AEA.

### Cell Transfection and Immunofluorescence

Cell transfection and double immunofluorescence techniques are detailed in Supplemental Data.

## SUPPLEMENTAL DATA

Supplemental Data include Supplemental Experimental Procedures and four figures and can be found with this article online at http://www.cell.com/chemistry-biology/supplemental/S1074-5521(09)00151-3.

## ACKNOWLEDGMENTS

The authors gratefully acknowledge E. Dainese for helpful discussions and A. Sabatucci for technical support. This investigation was partly supported by Fondazione TERCAS (Research Programs 2004 and 2005), by Ministero dell'Istruzione, dell'Università e della Ricerca (FIRB 2006), and by Agenzia Spaziale Italiana (DCMC project 2006). The authors have a patent filing on the biotin-anandamide used in this article. This patent has no financial association or relationship with any company.

Received: February 4, 2009
Revised: April 13, 2009
Accepted: May 7, 2009
Published online: May 28, 2009

## REFERENCES

Beltramo, M., Stella, N., Calignano, A., Lin, S.Y., Makriyannis, A., and Piomelli, D. (1997). Functional role of high-affinity anandamide transport, as revealed by selective inhibition. Science *277*, 1094–1097.

Berghuis, P., Dobszay, M.B., Wang, X., Spano, S., Ledda, F., Sousa, K.M., Schulte, G., Ernfors, P., Mackie, K., Paratcha, G., et al. (2005). Endocannabinoids regulate interneuron migration and morphogenesis by transactivating the TrkB receptor. Proc. Natl. Acad. Sci. USA *102*, 19115–19120.

Bojesen, I.N., and Hansen, H.S. (2003). Binding of anandamide to bovine serum albumin. J. Lipid Res. *44*, 1790–1794.

Breyer, E.D., Howard, S., Raje, N., Allison, S., Apkarian, R., Brown, W.V., and Strasters, J.K. (2003). Study of lipid and apolipoprotein binding interactions using vesicle affinity capillary electrophoresis. Anal. Chem. *75*, 5160–5169.

Casanova, M.L., Blazquez, C., Martinez-Palacio, J., Villanueva, C., Fernandez-Acenero, M.J., Huffman, J.W., Jorcano, J.L., and Guzman, M. (2003). Inhibition of skin tumor growth and angiogenesis *in vivo* by activation of cannabinoid receptors. J. Clin. Invest. *111*, 43–50.

Dainese, E., Oddi, S., Bari, M., and Maccarrone, M. (2007). Modulation of the endocannabinoid system by lipid rafts. Curr. Med. Chem. *14*, 2702–2715.

De Petrocellis, L., Bisogno, T., Davis, J.B., Pertwee, R.G., and Di Marzo, V. (2000). Overlap between the ligand recognition properties of the anandamide transporter and the VR1 vanilloid receptor: inhibitors of anandamide uptake with negligible capsaicin-like activity. FEBS Lett. *483*, 52–56.

Desarnaud, F., Cadas, H., and Piomelli, D. (1995). Anandamide amidohydrolase activity in rat brain microsomes. Identification and partial characterization. J. Biol. Chem. *270*, 6030–6035.

Deutsch, D.G., Glaser, S.T., Howell, J.M., Kunz, J.S., Puffenbarger, R.A., Hillard, C.J., and Abumrad, N. (2001). The cellular uptake of anandamide is coupled to its breakdown by fatty-acid amide hydrolase. J. Biol. Chem. *276*, 6967–6973.

Di Marzo, V. (2008). Targeting the endocannabinoid system: to enhance or reduce? Nat. Rev. Drug Discov. *7*, 438–455.

Drin, G., Mazel, M., Clair, P., Mathieu, D., Kaczorek, M., and Temsamani, J. (2001). Physico-chemical requirements for cellular uptake of pAntp peptide. Role of lipid-binding affinity. Eur. J. Biochem. *268*, 1304–1314.

Fegley, D., Kathuria, S., Mercier, R., Li, C., Goutopoulos, A., Makriyannis, A., and Piomelli, D. (2004). Anandamide transport is independent of fatty-acid amide hydrolase activity and is blocked by the hydrolysis-resistant inhibitor AM1172. Proc. Natl. Acad. Sci. USA *101*, 8756–8761.

Fezza, F., Oddi, S., Di Tommaso, M., De Simone, C., Rapino, C., Pasquariello, N., Dainese, E., Finazzi-Agrò, A., and Maccarrone, M. (2008). Characterization of biotin-anandamide, a novel tool for the visualization of anandamide accumulation. J. Lipid Res. *49*, 1216–1223.

Forneris, F., and Mattevi, A. (2008). Enzymes without borders: mobilizing substrates, delivering products. Science *321*, 213–216.

Fowler, C.J., Holt, S., Nilsson, O., Jonsson, K.O., Tiger, G., and Jacobsson, S.O. (2005). The endocannabinoid signaling system: pharmacological and therapeutic aspects. Pharmacol. Biochem. Behav. *81*, 248–262.

Fowler, C.J., Tiger, G., Ligresti, A., Lopez-Rodriguez, M.L., and Di Marzo, V. (2004). Selective inhibition of anandamide cellular uptake versus enzymatic hydrolysis–a difficult issue to handle. Eur. J. Pharmacol. *492*, 1–11.

Fuchs, E. (1990). Epidermal differentiation. Curr. Opin. Cell Biol. *2*, 1028–1035.

Furuhashi, M., and Hotamisligil, G.S. (2008). Fatty acid-binding proteins: role in metabolic diseases and potential as drug targets. Nat. Rev. Drug Discov. *7*, 489–503.

Gacad, M.A., and Adams, J.S. (1998). Proteins in the heat shock-70 family specifically bind 25-hydroxyvitamin D3 and 17beta-estradiol. J. Clin. Endocrinol. Metab. *83*, 1264–1267.

Gazzara, J.A., Phillips, M.C., Lund-Katz, S., Palgunachari, M.N., Segrest, J.P., Anantharamaiah, G.M., and Snow, J.W. (1997). Interaction of class A amphipathic helical peptides with phospholipid unilamellar vesicles. J. Lipid Res. *38*, 2134–2146.

Gehrmann, M., Liebisch, G., Schmitz, G., Anderson, R., Steinem, C., De Maio, A., Pockley, G., and Multhoff, G. (2008). Tumor-specific Hsp70 plasma membrane localization is enabled by the glycosphingolipid Gb3. PLoS ONE *3*, e1925.

Giuffrida, A., Rodriguez de Fonseca, F., and Piomelli, D. (2000). Quantification of bioactive acylethanolamides in rat plasma by electrospray mass spectrometry. Anal. Biochem. *280*, 87–93.

Glaser, S.T., Abumrad, N.A., Fatade, F., Kaczocha, M., Studholme, K.M., and Deutsch, D.G. (2003). Evidence against the presence of an anandamide transporter. Proc. Natl. Acad. Sci. USA *100*, 4269–4274.

Glaser, S.T., Kaczocha, M., and Deutsch, D.G. (2005). Anandamide transport: a critical review. Life Sci. *77*, 1584–1604.

  

Gorg, A., Obermaier, C., Boguth, G., Harder, A., Scheibe, B., Wildgruber, R., and Weiss, W. (2000). The current state of two-dimensional electrophoresis with immobilized pH gradients. Electrophoresis *21*, 1037–1053.

Hanada, K., Kumagai, K., Yasuda, S., Miura, Y., Kawano, M., Fukasawa, M., and Nishijima, M. (2003). Molecular machinery for non-vesicular trafficking of ceramide. Nature *426*, 803–809.

Hasse, S., Kothari, S., Rokos, H., Kauser, S., Schurer, N.Y., and Schallreuter, K.U. (2005). *In vivo* and *in vitro* evidence for autocrine DCoH/HNF-1alpha transcription of albumin in the human epidermis. Exp. Dermatol. *14*, 182–187.

Hillard, C.J., and Jarrahian, A. (2000). The movement of *N*-arachidonoylethanolamine (anandamide) across cellular membranes. Chem. Phys. Lipids *108*, 123–134.

Hillard, C.J., and Jarrahian, A. (2003). Cellular accumulation of anandamide: consensus and controversy. Br. J. Pharmacol. *140*, 802–808.

Ibdah, J.A., Krebs, K.E., and Phillips, M.C. (1989). The surface properties of apolipoproteins A-I and A-II at the lipid/water interface. Biochim. Biophys. Acta *1004*, 300–308.

Jacobsson, S.O., and Fowler, C.J. (2001). Characterization of palmitoylethanolamide transport in mouse Neuro-2a neuroblastoma and rat RBL-2H3 basophilic leukaemia cells: comparison with anandamide. Br. J. Pharmacol. *132*, 1743–1754.

Kaczocha, M., Hermann, A., Glaser, S.T., Bojesen, I.N., and Deutsch, D.G. (2006). Anandamide uptake is consistent with rate-limited diffusion and is regulated by the degree of its hydrolysis by fatty acid amide hydrolase. J. Biol. Chem. *281*, 9066–9075.

Kaczocha, M., Glaser, S.T., and Deutsch, D.G. (2009). Identification of intracellular carriers for the endocannabinoid anandamide. Proc. Natl. Acad. Sci. USA *106*, 6375–6380.

Katz, J., Bonorris, G., and Sellers, A.L. (1970). Extravascular albumin in human tissues. Clin. Sci. *39*, 725–729.

Klein, T.W. (2005). Cannabinoid-based drugs as anti-inflammatory therapeutics. Nat. Rev. Immunol. *5*, 400–411.

Lauckner, J.E., Jensen, J.B., Chen, H.Y., Lu, H.C., Hille, B., and Mackie, K. (2008). GPR55 is a cannabinoid receptor that increases intracellular calcium and inhibits M current. Proc. Natl. Acad. Sci. USA *105*, 2699–2704.

Leask, A., Rosenberg, M., Vassar, R., and Fuchs, E. (1990). Regulation of a human epidermal keratin gene: sequences and nuclear factors involved in keratinocyte-specific transcription. Genes Dev. *4*, 1985–1998.

Maccarrone, M., Bari, M., Lorenzon, T., Bisogno, T., Di Marzo, V., and Finazzi-Agrò, A. (2000). Anandamide uptake by human endothelial cells and its regulation by nitric oxide. J. Biol. Chem. *275*, 13484–13492.

Maccarrone, M., Di Rienzo, M., Battista, N., Gasperi, V., Guerrieri, P., Rossi, A., and Finazzi-Agrò, A. (2003). The endocannabinoid system in human keratinocytes. Evidence that anandamide inhibits epidermal differentiation through CB1 receptor-dependent inhibition of protein kinase C, activation protein-1, and transglutaminase. J. Biol. Chem. *278*, 33896–33903.

Mamelak, D., and Lingwood, C. (1997). Expression and sulfogalactolipid binding specificity of the recombinant testis-specific cognate heat shock protein 70. Glycoconj. J. *14*, 715–722.

Matsuda, L.A., Lolait, S.J., Brownstein, M.J., Young, A.C., and Bonner, T.I. (1990). Structure of a cannabinoid receptor and functional expression of the cloned cDNA. Nature *346*, 561–564.

McFarland, M.J., and Barker, E.L. (2004). Anandamide transport. Pharmacol. Ther. *104*, 117–135.

McFarland, M.J., Porter, A.C., Rakhshan, F.R., Rawat, D.S., Gibbs, R.A., and Barker, E.L. (2004). A role for caveolae/lipid rafts in the uptake and recycling of the endogenous cannabinoid anandamide. J. Biol. Chem. *279*, 41991–41997.

Menguy, T., Chenevois, S., Guillain, F., le Maire, M., Falson, P., and Champeil, P. (1998). Ligand binding to macromolecules or micelles: use of centrifugal ultrafiltration to measure low-affinity binding. Anal. Biochem. *264*, 141–148.

Moore, S.A., Nomikos, G.G., Dickason-Chesterfield, A.K., Schober, D.A., Schaus, J.M., Ying, B.P., Xu, Y.C., Phebus, L., Simmons, R.M., Li, D., et al. (2005). Identification of a high-affinity binding site involved in the transport of endocannabinoids. Proc. Natl. Acad. Sci. USA *102*, 17852–17857.

Munro, S., Thomas, K.L., and Abu-Shaar, M. (1993). Molecular characterization of a peripheral receptor for cannabinoids. Nature *365*, 61–65.

Oddi, S., Bari, M., Battista, N., Barsacchi, D., Cozzani, I., and Maccarrone, M. (2005). Confocal microscopy and biochemical analysis reveal spatial and functional separation between anandamide uptake and hydrolysis in human keratinocytes. Cell. Mol. Life Sci. *62*, 386–395.

Oddi, S., Fezza, F., Pasquariello, N., De Simone, C., Rapino, C., Dainese, E., Finazzi-Agrò, A., and Maccarrone, M. (2008). Evidence for the intracellular accumulation of anandamide in adiposomes. Cell. Mol. Life Sci. *65*, 840–850.

Ortar, G., Ligresti, A., De Petrocellis, L., Morera, E., and Di Marzo, V. (2003). Novel selective and metabolically stable inhibitors of anandamide cellular uptake. Biochem. Pharmacol. *65*, 1473–1481.

Ortega-Gutierrez, S., Hawkins, E.G., Viso, A., Lopez-Rodriguez, M.L., and Cravatt, B.F. (2004). Comparison of anandamide transport in FAAH wild-type and knockout neurons: evidence for contributions by both FAAH and the CB1 receptor to anandamide uptake. Biochemistry *43*, 8184–8190.

Paradisi, A., Pasquariello, N., Barcaroli, D., and Maccarrone, M. (2008). Anandamide regulates keratinocyte differentiation by inducing DNA methylation in a CB1 receptor-dependent manner. J. Biol. Chem. *283*, 6005–6012.

Piomelli, D. (2003). The molecular logic of endocannabinoid signalling. Nat. Rev. Neurosci. *4*, 873–884.

Rabilloud, T., Asselineau, D., and Darmon, M. (1988). Presence of serum albumin in normal human epidermis: possible implications for the nutrition and physiology of stratified epithelia. Presence of albumin in epidermis. Mol. Biol. Rep. *13*, 213–219.

Rakhshan, F., Day, T.A., Blakely, R.D., and Barker, E.L. (2000). Carrier-mediated uptake of the endogenous cannabinoid anandamide in RBL-2H3 cells. J. Pharmacol. Exp. Ther. *292*, 960–967.

Ruiz-Llorente, L., Ortega-Gutierrez, S., Viso, A., Sanchez, M.G., Sanchez, A.M., Fernandez, C., Ramos, J.A., Hillard, C., Lasuncion, M.A., Lopez-Rodriguez, M.L., et al. (2004). Characterization of an anandamide degradation system in prostate epithelial PC-3 cells: synthesis of new transporter inhibitors as tools for this study. Br. J. Pharmacol. *141*, 457–467.

Soccio, R.E., and Breslow, J.L. (2004). Intracellular cholesterol transport. Arterioscler. Thromb. Vasc. Biol. *24*, 1150–1160.

Starowicz, K., Nigam, S., and Di Marzo, V. (2007). Biochemistry and pharmacology of endovanilloids. Pharmacol. Ther. *114*, 13–33.

Sun, Y., and Bennett, A. (2007). Cannabinoids: a new group of agonists of PPARs. PPAR Res. *2007*, 23513.

Ueda, N., Okamoto, Y., and Morishita, J. (2005). N-acylphosphatidylethanolamine-hydrolyzing phospholipase D: a novel enzyme of the beta-lactamase fold family releasing anandamide and other *N*-acylethanolamines. Life Sci. *77*, 1750–1758.

Uittenbogaard, A., Ying, Y., and Smart, E.J. (1998). Characterization of a cytosolic heat-shock protein-caveolin chaperone complex. Involvement in cholesterol trafficking. J. Biol. Chem. *273*, 6525–6532.

Wang, H., Dey, S.K., and Maccarrone, M. (2006). Jekyll and hyde: two faces of cannabinoid signaling in male and female fertility. Endocr. Rev. *27*, 427–448.